Soft Matter

# Entropy-driven segregation in epoxy-amine systems at a copper interface



| | |
|---|---|
| Journal: | *Soft Matter* |
| Manuscript ID | SM-ART-09-2020-001600.R1 |
| Article Type: | Paper |
| Date Submitted by the Author: | 11-Nov-2020 |
| Complete List of Authors: | Yamamoto, Satoru; Kyushu University, Center for Polymer Interface and Molecular Adhesion Science<br>Tanaka, Keiji; Kyushu University, Department of Applied Chemistry |
| | |

ARTICLE

# Entropy-driven segregation in epoxy-amine systems at a copper interface

Received 00th January 20xx,
Accepted 00th January 20xx

DOI: 10.1039/x0xx00000x

Satoru Yamamoto*[a] and Keiji Tanaka*[abcd]

The composition of an epoxy resin at the interface with the adherend is usually different from that in the bulk due to the enrichment of a specific constituent, a characteristic called interfacial segregation. For better adhesion, it should be precisely understood how epoxy and amine molecules exist on the adherend surface and react with each other to form a three-dimensional network. In this study, the entropic factor of the segregation in a mixture of epoxy and amine at the copper interface before and after the curing reaction is discussed on the basis of a full-atomistic molecular dynamics (MD) simulation. Smaller molecules were preferentially segregated at the interface regardless of the epoxy and amine, and this segregation remained after the curing process. No segregation occurred at the interface for a combination composed of epoxy and amine molecules with a similar size. These findings make it clear that the size disparity between constituents affects the interfacial segregation via the packing and/or translational entropy. The curing reaction was slower near the interface than in the bulk, and a large amount of unreacted molecules remained there. Finally, the effect of molecular shape was also examined. Linear molecules were more likely to segregate than round-shaped ones even though they were similar in volume. We believe that these findings, which are difficult to obtain experimentally, contribute to the understanding of the interfacial adhesion phenomena on a molecular scale.

## 1. Introduction

The design of filler-containing composites is essentially based on the selection of a matrix and filler suitable for the application. At the same time, the interfacial adhesion between matrix and filler which strongly influences the thermal and mechanical properties and thereby the durability is also a key issue to be considered.[1-7] The surface modification of fillers[8-17] is a commonly adopted strategy for improving interfacial adhesion. In general, the filler surface is designed to work with the matrix via enthalpic interactions, considering compatibility based on the cohesive energy density. For example, dispersibility is improved by modifying the surface of nanofillers to be either hydrophilic or hydrophobic according to the matrix.[14,17,18] It is therefore of pivotal importance to obtain a better understanding of how the filler surface and matrix interact at the molecular level.

Epoxy resin which is a class of typical thermosetting resins is expected to be used as a structural adhesive for the automobile and aviation industries as well as a precise adhesive bonding and sealing resin for the electrics industry thanks to its excellent adhesive strength, high stiffness and light weight.[19-26] Epoxy and amine compounds with various molecular structures are generally used as a base resin and curing agent, respectively, and the combination is determined on the basis of the application of the cured resin. They are stoichiometrically mixed to promote the cross-linking reaction between epoxy and amino groups. The rigid three-dimensional network so formed plays an important role in material properties such as the modulus, adhesive properties, thermal expansion, and fracture behavior.[27-32] Thus, to improve the adhesive performance with the adherend, for example, fillers for composite materials as well as metals and wafers for electronic packaging, it is essential to understand the detailed molecular picture and successive reaction process to form the network structure at and near to the interfaces.

The composition of a mixture at the interface is usually different from that in the bulk due to the enrichment of a specific component. Such segregation can be promoted by both enthalpic and entropic factors to minimize the free energy at the interface.[33-39] The enthalpy-driven segregation is easy to understand intuitively as the compatibility is based on the cohesive energy density, and the material is often designed based on this factor. The entropic attraction toward the interface should also play an important role in the mixture. This is the case even for linear polymers because of the favourable existence of shorter chains at the interface due to this factor in terms of conformational, translational, or packing, depending on which aspect is the focus.[40-42] In our earlier report on an epoxy-amine mixture via both experimentation[43,44] and simulation[45] in which the average composition was adjusted to

[a] Centre for Polymer Interface and Molecular Adhesion Science, Kyushu University, Fukuoka 819-0395, Japan. E-mail: s-yamamoto@cstf.kyushu-u.ac.jp
[b] Department of Applied Chemistry, Kyushu University, Fukuoka 819-0395, Japan. E-mail: k-tanaka@cstf.kyushu-u.ac.jp
[c] Department of Automotive Science, Kyushu University, Fukuoka 819-0395, Japan.
[d] International Institute for Carbon-Neutral Energy Research (WPI-I2CNER), Kyushu University, Fukuoka 819-0395, Japan.

† Electronic Supplementary Information (ESI) available: Simulation details for a quaternary system and binary mixture systems after the curing reaction. See DOI: 10.1039/x0xx00000x

the stoichiometric ratio, an excess amount of amine molecules that were smaller than epoxy existed at the interface, which was neutral in charge, owing to the entropic factor. Although there are no such reports dealing with the interfacial segregation of the epoxy component, it should also be segregated under entropically favorable conditions where the energetic, or enthalpic, factor is relatively smaller. Tackling this point leads to an understanding of how the epoxy and amine agents are present on the adherend surface and how they move around dynamically and react with each other to form the three-dimensional network. This should thereby result in the better adhesion of epoxy resins.

In this study, from the perspective of the entropic factor, we investigated how the molecular size influenced the interfacial segregation based on a full-atomistic molecular dynamics (MD) simulation using various combinations with two different size epoxy and amine molecules.[46-58] In addition, the interfacial segregation was further investigated using a combination of constituents which were identical in size but different in shape. Although a full-atomistic MD simulation is suitable for this kind of research, the number of atoms handled is generally limited. This drawback was overcome herein by performing the simulation with a narrow gap sandwiched between two copper layers, which was sufficient to shed a light near the solid interface.[45] The information at the molecular level obtained here will help to understand the adhesive interface phenomena and lead to the development of adhesives with better performance.

## 2. Simulation method

### 2.1 Materials

Fig. 1 shows the chemical structures of diglycidyl ether of bisphenol-A (referred to as Ep-L), ethylene glycol diglycidyl ether (Ep-S), 2,2-di(4-(3-aminopropyl)phenyl)propane (Am-L), and 1,8-diaminooctane (Am-S) as large/small epoxy and amine molecules, respectively. Their molecular weights and volumes are summarized in Table 1. The volume was estimated based on the surface which was the boundary between a 0.14 nm probe, which was approximately the radius of a water molecule, and atoms.[59] Larger molecules are roughly twice the size of the smaller ones.

**Table 1** Molecular weight (*Mw*) and volume (*Vm*) of components.

| | Ep-L | Ep-S | Am-L | Am-S |
|---|---|---|---|---|
| *Mw* | 340 | 174 | 310 | 144 |
| *Vm* ($nm^3$) | 0.344 | 0.179 | 0.359 | 0.176 |

### 2.2 Simulation system

All calculations reported in this study were performed using the Materials Studio 2020 (Dassault Systèmes) software package. Using a confined space of a 15 nm gap sandwiched between two copper (1 1 1) surfaces with an area of 3.1 × 3.1 $nm^2$ and a thickness of 1.9 nm as shown in Fig. 1, the segregation phenomenon for the mixture at the copper interface was investigated via a full-atomistic MD simulation before and after the curing process. The size of the copper surface was chosen to maintain computational performance, and its plausibility was confirmed comparing with a result with a 6 × 6 $nm^2$ copper substrate.[45] A Forcite module was used with a COMPASS II forcefield[60-62] under an NVT ensemble using a Nose-Hoover-Langevin (NHL) thermostat, after determining the equilibrium density under the NPT ensemble. The gap size of 15 nm for the simulation was sufficient to avoid the thinning effect on the interfacial segregation phenomenon.[45] A copper surface was chosen because it is often used as a substrate for epoxy resins and the interface has been well characterized experimentally.[44]

To create the initial structure for each combination of epoxy and amine, an Amorphous Cell module using the Monte Carlo method was used. The mixture of epoxy and amine molecules with a stoichiometric ratio was introduced into the gap with a density of 1.09, 1.08, 1.07, and 1.02 $g \cdot cm^{-3}$ for the Ep-L/Am-L, Ep-L/Am-S, Ep-S/Am-L, and Ep-S/Am-S combinations, respectively. These densities were obtained at an equilibrium state for 100 epoxy and 50 amine molecules in the cubic cell after a 1 ns MD simulation under the fully periodic boundary condition for the NPT ensemble at 1 atm and 296 K. Although the density increased after the reaction proceeded due to the formation of the cross-linked structure by at most a few percent, the MD simulation was here conducted under the NVT ensemble. This was because the NPT ensemble could not be adopted as the specification of the MD module used under a condition that the copper layer was constrained. Thus, it was pre-confirmed that the reaction kinetics was essentially the

**Table 2** Number of constituent molecules for the simulation systems.

| epoxy/amine | epoxy molecules | amine molecules | total atoms of epoxy/amine |
|---|---|---|---|
| Ep-L/Am-L | 188 | 94 | 14,194 |
| Ep-L/Am-S | 224 | 112 | 14,336 |
| Ep-S/Am-L | 280 | 140 | 14,700 |
| Ep-S/Am-S | 356 | 178 | 14,596 |

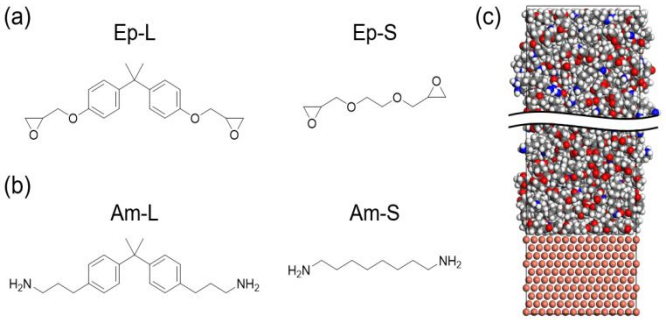


**Fig. 1** Chemical structures of (a) epoxy and (b) amine molecules, and (c) a simulation system with a cell size of 3.1 × 3.1 × 16.9 $nm^3$, which is composed of an epoxy-amine mixture confined in a 15 nm-thick gap between the copper layers with a total thickness of 1.9 nm, under a periodic boundary condition. Carbon, oxygen, nitrogen, hydrogen and copper atoms are colored gray, red, blue, white and brown, respectively.

same for both NVT and NPT ensembles. Table 2 shows the number of constituent molecules and the total number of atoms for the simulation excluding copper layers. The number of copper atoms was fixed at 1,680 and the copper layers were constrained during the simulation. A 1 ns simulation was run to investigate the structural and dynamic properties of the system before the curing process. All calculations were run for ten different initial structures and then averaged.

### 2.3 Curing process

The curing reactions of the epoxy-amine system were performed via the MD simulation.[52,55] If an epoxy group approaches an amino group within the reaction range set at 0.4 nm, a reaction may occur resulting in the formation of a cross-linking point. The judgement of whether or not a reaction had occurred was based on the comparison between a reaction probability composed of the frequency factor and the activation energy with the local absolute temperature and a random number. Since the purpose of this study was to examine the size disparity effect for the constituents on the interfacial segregation, the activation energies were set to be equal for all systems, 56.8 and 55.3 kJ · mol$^{-1}$ for the 1$^{st}$ and 2$^{nd}$ reactions, respectively. The heat of formation was also set to 58.6 kJ · mol$^{-1}$ for both reactions in all systems, following our previous differential scanning calorimetry (DSC) results.[44] To analyze the reaction process of the mixture in detail, the curing reaction was monitored at 296 K, which was the same as our previous experiment,[44] for 10 ns. While the data for before the curing reaction were averaged over ten simulation runs, the results from three different initial structures were averaged for the curing process.

## 3. Results and discussion

### 3.1 Interfacial aggregation states

Fig. 2 shows the density profiles for Ep-L/Am-L, Ep-L/Am-S, Ep-S/Am-L, and Ep-S/Am-S with a sampling interval of 0.05 nm. The position is defined along the direction perpendicular to the copper surface, and the positions of 0 and 15 nm correspond to the bottom and top interfaces, respectively. As a trend common to all systems, the density near the interface was higher than in the internal region. It asymptotically reached the bulk value while oscillating toward the internal region. The thicknesses of the interfacial region where the density oscillation appeared were 1.3, 1.4, 1.9, and 2.6 nm for Ep-L/Am-L, Ep-L/Am-S, Ep-S/Am-L, and Ep-S/Am-S, respectively. For instance, in the case of Ep-L/Am-S which was a combination of the larger epoxy and smaller amine components, as shown in panel (b), although the density was 1.08 g·cm$^{-3}$ averaged over the entire region, it was maximized to 1.8 g·cm$^{-3}$ very near to both the bottom and top interfaces and minimized to 0.8 g·cm$^{-3}$ at the adjacent region located on the opposite side to the interface. The second maximum was also observed around 1 nm from the interface. This density oscillation was the least and most striking for the Ep-L/Am-L and Ep-S/Am-S systems, which were the combinations of both larger constituents and both smaller ones, respectively, as shown in panels (a) and (d). In all systems, although epoxy and amine molecules existing near the interface basically oriented parallel to the copper wall, as shown in Figs. S1 and S2 (see ESI†),[45,63,64] there were also some randomly-oriented molecules. The presence of randomly-oriented molecules disturbed the interfacial ordering and the degree was more remarkable for larger molecules than for smaller one.[65]

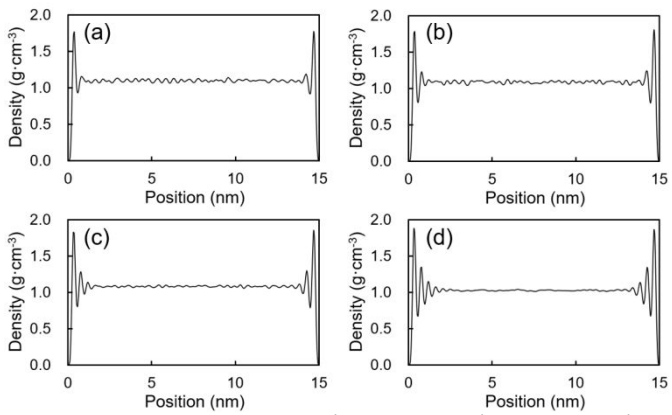


**Fig. 2** Density profiles of (a) Ep-L/Am-L, (b) Ep-L/Am-S, (c) Ep-S/Am-L, and (d) Ep-S/Am-S mixtures along the perpendicular direction to the copper interface. The 0 and 15 nm positions correspond to the bottom and top interfaces, respectively.

Fig. 3 shows the position dependent relative number density of epoxy and amine molecules for all mixtures. The average values for epoxy and amine should be 2 and 1, respectively, according to the stoichiometry. As a general trend for all combinations, both epoxy and amine were enriched at the interface compared with the interior region. The amount of amine was divided by that of epoxy so that the particular component and to what extent it was segregated at the interface could be discussed. Fig. 4 shows the results of the analysis of data depicted in Fig. 3. The molar ratio of amine to epoxy was 0.5 on average in the internal region for all systems, meaning that both existed in stoichiometric quantities. In panel (a) for the Ep-L/Am-L system, the ratio was 0.56±0.07 even at the interface, almost maintaining the stoichiometric ratio. On

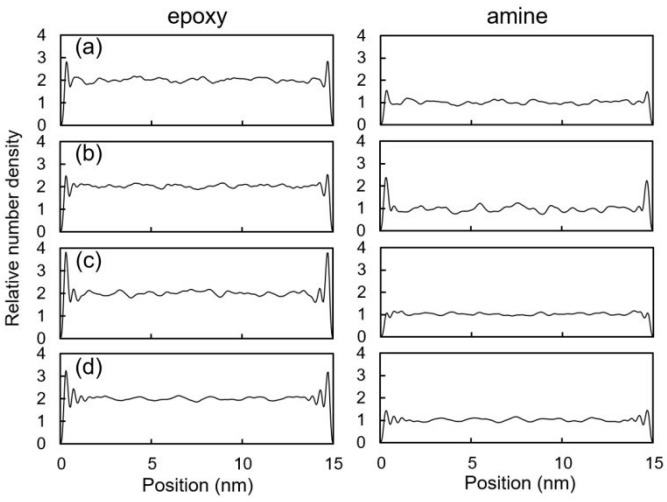


**Fig. 3** Relative number densities of epoxy and amine molecules in (a) Ep-L/Am-L, (b) Ep-L/Am-S, (c) Ep-S/Am-L, and (d) Ep-S/Am-S mixtures. Initial relative number densities were 2 for epoxy and 1 for amine.

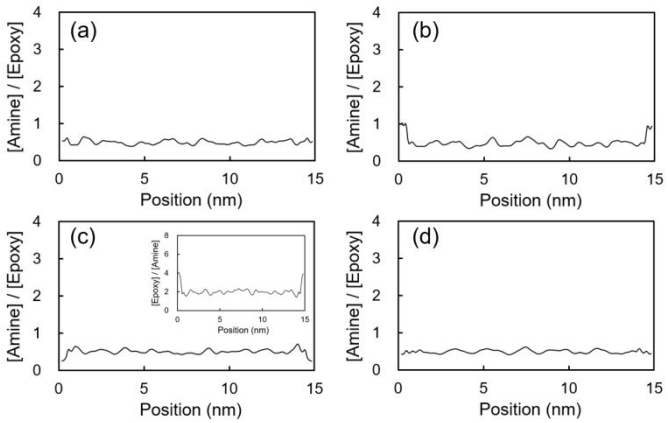


**Fig. 4** Molar ratios of amine to epoxy for (a) Ep-L/Am-L, (b) Ep-L/Am-S, (c) Ep-S/Am-L, and (d) Ep-S/Am-S mixtures with a bulk ratio of 0.5. The inset in panel (c) shows the same data as the main panel but with the molar ratio of epoxy to amine in which a bulk ratio was 2.0 on average.

the other hand, in the case of the Ep-L/Am-S system shown in panel (b), the ratio was 0.97±0.15 at the interface. This makes it clear that there was an excess amount of amine at the interface. In contrast, for Ep-S/Am-L in panel (c), the ratio was smaller than 0.5 near the interface. For clarification therefore, the ratio of epoxy to amine is taken on the ordinate in the inset of panel (c), which is the opposite of that in the main panel, and in this case, the stoichiometric value is supposed to be 2.0 on average. The molar ratio of epoxy to amine reached 3.71±0.80, meaning that the epoxy component was segregated at the copper interface for the Ep-S/Am-L system as opposed to the Ep-L/Am-S system.

In the current simulations, only van der Waals forces were counted for the attraction of the epoxy and amine molecules due to the lack of charge on the copper surface, implying that the interactions were of a similar magnitude for all molecules. This was verified by comparing the density profile of each constituent on the copper surface with those of others as well as the mixtures.[63] Thus, it seems most likely that the interfacial segregation of Am-S and Ep-S shown in Fig. 4 (b) and (c), respectively, was driven by the size disparity, or packing and translational entropy.[40,42] Finally, in the Ep-S/Am-S system as shown in panel (d), the molar ratio of amine to epoxy was maintained at 0.5 throughout the system and was 0.51±0.05 even near the interface. Therefore, such an entropy-driven segregation was not clearly discernable in panels (a) and (d) in which the constituents of epoxy and amine were of a comparable size to each other.

In industry, to regulate the physical properties of thermosetting resins, the reaction mixture is prepared by multiple constituents. Thus, the following describes what happens with the interfacial segregation when the two epoxy and two amine molecules used in this study are mixed together. A simulation system consisting of 272 epoxy and 136 amine molecules, or a mixture of 94 Ep-L, 178 Ep-S, 47 Am-L, and 89 Am-S, was constructed. The number of the constituent molecules was determined so that the amount of Ep-L/Am-L and Ep-S/Am-S systems became equal to each other by mixing them. The density of this quaternary mixture increased near the interface in a similar manner to the binary one, as shown in Fig. S5 (see ESI†). Similar to the binary mixture, the relative number density of epoxy and amine molecules was analyzed as a function of the position from the copper interface for the quaternary mixture, as shown in Fig. S6 (see ESI†). However, it was difficult only from this figure to judge whether the interfacial segregation of the constituent/s occurred. The relationship between the relative amount and the distance from the interface was then divided into each constituent. Fig. 5 shows the relative number densities of (a) epoxy and (b) amine molecules as a function of the position for all constituents. This clearly indicates that the smaller constituents of both epoxy and amine, namely Ep-S and Am-S, respectively, were selectively segregated at the interface. On the other hand, the amount of the larger molecules of epoxy and amine, Ep-L and Am-L, respectively, at the interface was comparable to the average one. To facilitate intuitive understanding, a snapshot of the cell containing constituents in the vicinity of the interface is shown in panel (c). This was obtained by an additional 1 ns MD calculation on a supercell with an area of 6.2 × 3.1 nm$^2$, which was doubled in width for the sake of clarity. It is clear that Ep-S and Am-S were preferentially segregated at the interface.

In panels (a) and (b), the relative number density of the smaller epoxy and amine constituents, Ep-S and Am-S, at the interface increased twofold from the average value of 2 to 4 and 1 to 2, respectively. Therefore, it can be claimed that the effects of segregation of epoxy and amine having the same size are similar.

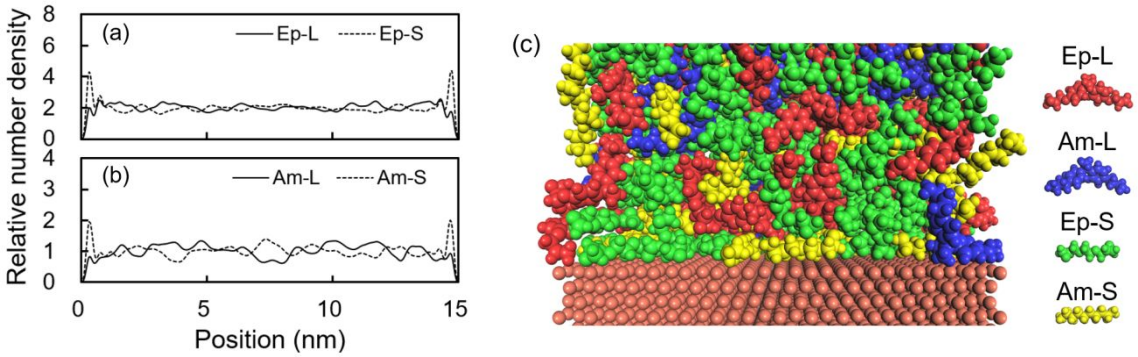


**Fig. 5** Relative number densities of (a) epoxy and (b) amine molecules. Initial relative number densities were 2 for epoxy and 1 for amine. (c) A representative snapshot of a supercell with an area of 6.2 × 3.1 nm$^2$ near the interface. Molecules of Ep-L, Am-L, Ep-S, and Am-S are colored red, blue, green and yellow, respectively. Copper atoms are colored brown.

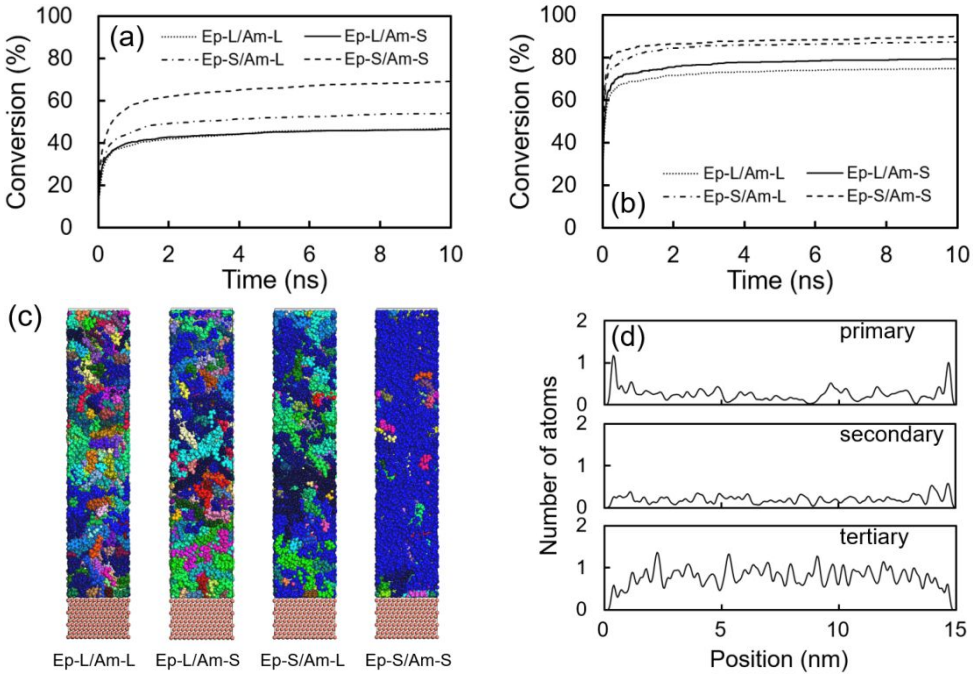


**Fig. 6** Time course of reaction conversions for various combinations of epoxy and amine molecules in (a) the confined system between copper layers and (b) the bulk system with periodic boundaries. (c) Snapshots of the microstructure at 10 ns. Each color represents an isolated fragment which is connected via chemical bonds. (d) Distribution of primary, secondary, and tertiary amine molecules in the Ep-S/Am-S system.

### 3.2 Curing process

Fig. 6 (a) shows the time course of the reaction conversion for Ep-L/Am-L, Ep-L/Am-S, Ep-S/Am-L and Ep-S/Am-S in the gap with a thickness of 15 nm sandwiched between the copper surfaces. The conversion was derived from the consumption ratio of epoxy molecules. The results of the bulk system, consisting of 100 epoxy and 50 amine molecules in a cubic unit cell with fully periodic boundary conditions, are also shown in Fig. 6 (b) for comparison. The overall trend was that the reaction proceeded more slowly in the confined states than in the bulk ones probably due to the inhibition of the molecular motion in close proximity to the copper walls and thereby the depletion of a reaction partner.[45,65] This explanation was verified by the reaction conversion profiles, as shown in Fig. S11 (see ESI†), and good accordance with our knowledge for polymer systems.[66,67] In the bulk, the percolated network structure, which was three-dimensionally connected via chemical bonds, was formed in the entire cell for all combinations. The combination of smaller reactants, Ep-S/Am-S, reached the highest conversion both in the confined and bulk systems, and the reaction conversions after 10 ns were 69.3±1.9 % and 90.2±1.3 %, respectively.

Fig. 6 (c) shows snapshots of the microstructure for each combination in the confined state after 10 ns-reaction. An isolated fragment developed via chemical bonds is drawn by a color. In the case of the Ep-S/Am-S system, a fragment percolating from the bottom to the top interface, indicated in blue, was discernable even though small fragments remained in some places. The system which attained the second highest conversion was Ep-S/Am-L, and the conversions for the confined and bulk states were 54.0±1.4 % and 87.3±1.2 %, respectively. The two systems of Ep-L/Am-L and Ep-L/Am-S exhibited lower conversions both in confined and bulk states. The values after 10 ns were 47.0±0.8 % and 74.8±3.8 % for Ep-L/Am-L and 46.7±1.3 % and 79.7±1.5 % for Ep-L/Am-S, respectively. Except the Ep-S/Am-S system, the percolating structure throughout the entire region was not observed.

Here, the aggregation states of constituents in the confined system, which are the density (Fig. S7 (see ESI†)), the relative concentration of epoxy and amine molecules (Fig. S8 (see ESI†)), the molecular ratio of amine to epoxy (Fig. S9 (see ESI†)), and the relative concentration of primary, secondary and tertiary amines (Fig. S10 (see ESI†)), at the copper interface after the reaction of 10 ns are briefly stated. Comparing these with the results shown in Figs. 2, 3, and 4, it is conceivable that the density increase, segregation of epoxy and amine, and deviation of the molecular ratio of amine to epoxy at the interface were essentially the same as before the reaction. Although the conversions reached after 10 ns-reaction differed from one

**Table 3** Self-diffusion coefficients of epoxy and amine molecules in the bulk for four epoxy/amine systems before the curing reaction.

| epoxy-amine | $D_{epoxy}$ ($10^{-10}$ $m^2 \cdot s^{-1}$) | $D_{amine}$ ($10^{-10}$ $m^2 \cdot s^{-1}$) |
|---|---|---|
| Ep-L/Am-L | 0.13±0.01 | 0.14±0.02 |
| Ep-L/Am-S | 0.20±0.03 | 0.37±0.11 |
| Ep-S/Am-L | 0.56±0.44 | 0.31±0.20 |
| Ep-S/Am-S | 2.08±0.35 | 2.17±0.46 |

another, the unreacted primary amine was localized in close proximity to the interface for all systems, as shown in Fig. S10 (see ESI†). Even in the Ep-S/Am-S system which reached the highest reaction conversion and formed the percolated network, the peak of primary amines was observed near the interface, as shown in Fig. 6 (d). This implies that the reaction was suppressed near the copper wall due to the decrease in mobility of molecules and the depletion of reaction partners.

Comparing two combinations composed of larger and smaller molecules such as Ep-L/Am-S and Ep-S/Am-L, the system with smaller epoxy molecules reacted faster both in the confined and bulk states. To better understand this phenomenon, the dynamic feature of epoxy and amine molecules was examined. Table 3 lists bulk self-diffusion coefficients of constituents for four epoxy/amine combinations, provided that these values represent the mobility before the reaction. Ep-S and Am-S in their combination exhibited the largest self-diffusion coefficients as epoxy and amine molecules, and thus reacted promptly. On the other hand, the diffusion coefficients of larger epoxy and amine molecules in their combination, Ep-L/Am-L, were the smallest. The point that should be noted is that Ep-S mixed with Am-L moved more slowly than that mixed with Am-S. This indicates that when a certain molecule is mixed with a slow-moving larger molecule, the self-diffusion coefficient is lower than that for the same molecule mixed with a fast-moving smaller molecule. The "matrix" effect greatly impacts the kinetics of the successive reactions in the epoxy and amine mixture.

An epoxy group reacts once, whereas an amino group reacts twice. Once an amino group reacts with an epoxy group, it is incorporated into a part of the product and must then wait for another epoxy to approach. Although the product itself can move before the vitrification occurs, the mobility is much slower than that of an unreacted epoxy molecule, leading to a situation where the amine incorporated in the product looks to be relatively immobile. This matrix effect is supposed to be amplified as the reaction proceeds and is consistent with the simulation results shown in Figs. 6 (a) and (b). Since the discussion is important in considering competitive multi-step reactions in thermosetting resins, this hypothesis is further studied in the near future, changing the mobility of molecules in the reaction process.

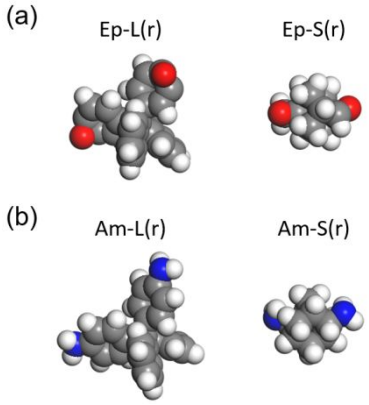


**Fig. 7** Space-filling models of round-shaped larger/smaller (a) epoxy and (b) amine molecules. Carbon, oxygen, nitrogen and hydrogen are colored gray, red, blue and white, respectively.

### 3.3 Molecular shape effect

In the above, it was reported that the size disparity between/among constituents is one of the important controlling factors in the aggregation states of thermosetting resins at the interface. This entropy-driven segregation can be understood on the basis of the packing and/or the translation of molecules at the interface. Thus, even if the sizes of epoxy and amine are comparable to each other, it seems reasonable to predict that the interfacial segregation is promoted by the unique molecular shape of one of the constituents. To confirm this hypothesis, calculations were performed using a combination of linear and round-shaped molecules.

Fig. 7 shows space-filling models of round-shaped larger/smaller (a) epoxy and (b) amine molecules such as 3,3'-(diphenylmethanediyl)bis(7-oxabicyclo[4.1.0]hepta-1,3,5-triene) (referred to as Ep-L(r)), 4'-oxaspiro(oxirane-2,9'-tetracyclo[4.3.1.1$^{3,8}$.0$^{3,5}$]undecane) (Ep-S(r)), 4,4'-(diphenylmethanediyl)dianiline (Am-L(r)), and adamantane-2,6-diamine (Am-S(r)). The molecular volumes of Ep-L(r), Ep-S(r), Am-L(r), and Am-S(r) were 0.345, 0.183, 0.368, and 0.181 nm$^3$, respectively. These volumes are comparable to those of the linear epoxy and amine molecules listed in Table 1. They were independently mixed with the linear epoxy or amine molecules with a corresponding size; Ep-L/Am-L(r), Ep-L(r)/Am-L, Ep-S/Am-S(r), and Ep-S(r)/Am-S. The mixtures consisted of 190 Ep-L and 95 Am-L(r), 194 Ep-L(r) and 97 Am-L, 368 Ep-S and 184 Am-S(r), and 360 Ep-S(r) and 180 Am-S molecules, respectively, and the numbers of molecules were determined from the equilibrium density of 1.14, 1.14, 1.10, and 1.05 g·cm$^{-3}$ at 296 K.

Fig. 8 shows the relative number densities of epoxy and amine molecules in Ep-L/Am-L(r), Ep-L(r)/Am-L, Ep-S/Am-S(r), and Ep-S(r)/Am-S as a function of position obtained from 1 ns simulation. In panels (a) and (c), the density of epoxy was noticeably higher near to the copper wall than in the internal region. This indicates that the linear epoxy components, Ep-L

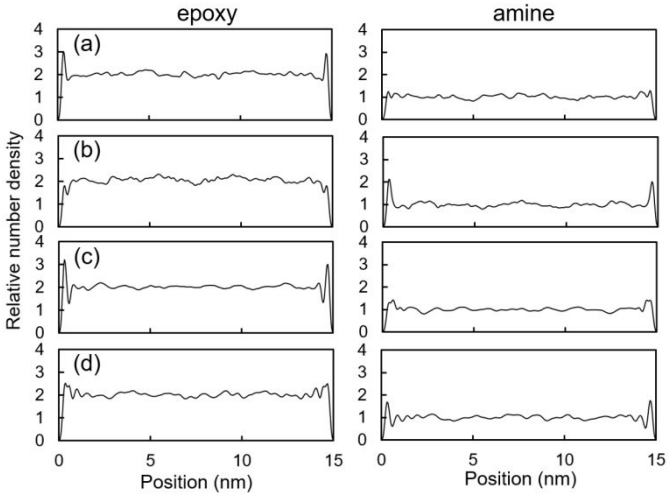


**Fig. 8** Relative number densities of epoxy and amine molecules in (a) Ep-L/Am-L(r), (b) Ep-L(r)/Am-L, (c) Ep-S/Am-S(r), and (d) Ep-S(r)/Am-S. The average density was set to 2 for epoxy and 1 for amine in all systems.

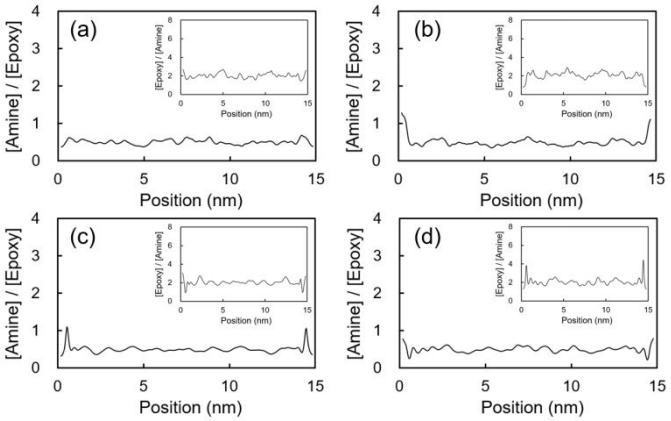


**Fig. 9** Molar ratios of amine to epoxy for (a) Ep-L/Am-L(r), (b) Ep-L(r)/Am-L, (c) Ep-S/Am-S(r), and (d) Ep-S(r)/Am-S mixtures with a bulk ratio of 0.5. The insets show the same data as the main panel but with the molar ratio of epoxy to amine in which a bulk ratio was 2.0 on average.

and Ep-S, were selectively segregated at the interface. Similarly, in panels (b) and (d), the density of amine, which was a linear component, was higher at the interface. In all systems, linear-shaped molecules existing near the interface were strongly oriented parallel to the copper wall, as shown in Figs. S3 and S4 (see ESI†).[45,63,64] The enthalpic interaction with the wall surface was slightly greater for linear-shaped molecules than for round-shaped one. However, as seen in the snapshots (Fig. S4 (see ESI†)), round-shaped molecules were not tightly packed at the interface, whereas linear ones were. Thus, the interfacial segregation of the linear component can be explained in terms of the packing of molecules, namely the entropy, at the interface.

Fig. 9 shows the molar ratio of amine to epoxy calculated from the data depicted in Fig. 8. In the combination of larger molecules, the molar ratios of amine to epoxy at the copper interface were 0.46±0.15 (2.60±0.89) and 1.45±0.69 (1.01±0.31) for the Ep-L/Am-L(r) and Ep-L(r)/Am-L systems, respectively. The number in parentheses is the inverse of the ratio, or the molar ratios of epoxy to amine. Taking into account the bulk amine/epoxy ratio of 0.5 (the inverse ratio of 2.0), it is apparent that Ep-L and Am-L were segregated at the copper interface in the Ep-L/Am-L(r) and Ep-L(r)/Am-L mixture, respectively. Similarly, in the combination of smaller molecules, the molar ratios of amine to epoxy at the interface were 0.41±0.09 (2.87±0.80) and 0.76±0.10 (1.54±0.14) for the Ep-S/Am-S(r) and Ep-S(r)/Am-S systems, respectively. This indicates that Ep-S and Am-S were preferentially segregated at the interface in these two systems. It is also notable that peaks were observed at positions adjacent to the interface in the main panel of Fig. 9 (c). This means that a linear component was depleted in the adjacent region on the opposite side of the interface, where the linear component was segregated. This was because the density oscillation was clearly observable for the combination of smaller molecules, as shown in Fig. 2 (d). That is, the layered structure was formed near the interface in this case so that the segregation of one component might cause the depletion of the component in the adjacent region. Therefore, it can be claimed that the segregation in the epoxy/amine system at the interface is tunable based on the molecular shape in addition to the molecular size.

## 4. Conclusions

The aggregation states for stoichiometric mixtures of epoxy and amine molecules with two different sizes at a copper interface were studied via a full-atomistic MD simulation so that the effect of the size disparity of the constituents on interfacial segregation could be discussed. The mixture was confined to a 15 nm-thick gap between two copper walls and dynamically simulated using a Forcite module of Materials Studio 2020 with the COMPASS II forcefield under the NVT ensemble using an NHL thermostat after determining the equilibrium density under the NPT ensemble. As a general trend, the density was much higher in close proximity to the interface than in the internal region of the gap. When epoxy was smaller than amine, an excess amount of epoxy was present at the copper interface and vice-versa. On the other hand, no interfacial segregation occurred for the mixtures of epoxy and amine with a similar size. Since the enthalpic interactions of epoxy and amine with the copper surface were identical to each other, it was claimed that the segregation was promoted by the size disparity between the constituents via packing and/or translational entropy at the interface. Even when the epoxy/amine mixture was expanded to the quaternary system, the smallest constituent was enriched at the interface. The final challenge was undertaken using a binary mixture in which the constituents were identical in volume but different in molecular shape. In this case, the linear constituent was segregated at the interface rather than the round-shaped one. These results demonstrate that the entropy-driven interfacial segregation is universal for the epoxy/amine system if the enthalpy contribution is small enough, that is, in the absence of the strong electrostatic interaction. With respect to the curing process, the system of both smaller epoxy and amine reached the highest conversion due to their higher mobility, whereas the conversion for the combination of both larger epoxy and amine was the lowest. Also, the size effect on the reaction kinetics was more striking for epoxy than amine in the curing process. This was because while an epoxy group reacts once, an amino group reacts twice. The amino group once reacted with an epoxy molecule was incorporated into the product and had to wait for another epoxy to approach due to the relatively lower mobility, or larger size. We believe that the findings in this study are useful for understanding interfacial phenomena and designing better adhesives from the viewpoint of the molecular picture at the interface.

## Conflicts of interest

There are no conflicts to declare.

## Acknowledgements

The authors thank R. Kuwahara (Dassault Systèmes K. K.) for helpful comments and discussions. This research was supported by JST-Mirai Program (JPMJMI18A2).

## Notes and references

1. C. Calvino, N. Macke, R. Kato and S. J. Rowan Development, *Prog. Polym. Sci.*, 2020, **103**, 101221.
2. Y. Fan, G. D. Fowler and M. Zhao, *J. Clean. Prod.*, 2020, **247**, 119115.
3. M. M. Adnan, E. G. Tveten, J. Glaum, M.-H. G. Ese, S. Hvidsten, W. Glomm and M.-A. Einarsrud, *Adv. Electron. Mater.*, 2019, **5**, 1800505.
4. R. Rohini, P. Katti and S. Bose, *Polymer*, 2018, **70**, A17–A34.
5. Z. Martín, I. Jiménez, M. A. Gómez-Fatou, M. West and A. P. Hitchcock, *Macromolecules*, 2018, **44**, 2179–2189.
6. M. J. Arlen, D. Wang, J. D. Jacobs, R. Justice, A. Trionfi, J. W. P. Hsu, D. Schaffer, L.-S. Tan and R. A. Vaia, *Macromolecules*, 2008, **41**, 8053–8062.
7. P. Zhang, J. Zeng, S. Zhai, Y. Xian, D. Yang and Q. Li, *Macromol. Mater. Eng.*, 2017, **302**, 1700068.
8. S. Sugimoto, M. Inutsuka, D. Kawaguchi and K. Tanaka, *Polym. J.*, 2020, **52**, 217–223.
9. E. I. Akpan, B. Wetzel and K. Friedrich, *J. Appl. Polym. Sci.*, 2020, **137**, 48719.
10. T. Shui, B. B. Adhikari, M. C. Chae and D. C. Bressler, *Prog. Org. Coat.*, 2020, **140**, 105535.
11. K. Yamamoto, D. Kawaguchi, K. Sasahara, M. Inutsuka, S. Yamamoto, K. Uchida, K. Mita, H. Ogawa, M. Takenaka and K. Tanaka, *Polym. J.*, 2019, **51**, 247–255.
12. Y. Fukunaga, Y. Fujii, S. Inada, Y. Tsumura, M. Asada, M. Naito and N. Torikai, *Polym. J.*, 2019, **51**, 275–281.
13. Y. Shinohara, H. Kishimoto, T. Masui, S. Hattori, N. Yamaguchi and Y. Amemiya, *Polym. J.*, 2019, **51**, 161–171.
14. A.-C. Genix, C. Schmitt-Pauly, J. G. Alauzun, T. Bizen, P. H. Mutin and J. Oberdisse, *Macromolecules*, 2017, **50**, 7721–7729.
15. M. Cvek, M. Mrlík, M. Ilčíková, J. Mosnáček and L. Münster, *Macromolecules*, 2017, **50**, 2189–2200.
16. K. W. Stöckelhuber, A. S. Svistkov, A. G. Pelevin and G. Heinrich, *Macromolecules*, 2011, **44**, 4366–4381.
17. E. D. Laird and C. Y. Li, *Macromolecules*, 2011, **46**, 2877–2891.
18. A. F. Ghanem, A. M. Youssef and M. H. A. Rehim, *J. Mater. Sci.*, 2020, **55**, 4685–4700.
19. R. Aoki, A. Yamaguchi, T. Hashimoto, M. Urushisaki, T. Sakaguchi, K. Kawabe, K. Kondo and H. Iyo, *Polym. J.*, 2019, **51**, 909–920.
20. S. Chen, Z. Xu and D. Zhang, *Chem. Eng. J.*, 2018, **343**, 283–302.
21. F. Snijkers, R. Pasquino and A. Maffezzoli, *Soft Matter*, 2017, **13**, 258–268.
22. M. Naebe, J. Wang, A. Amini, H. Khayyam, N. Hameed, L. H. Li, Y. Chen and B, Fox, *Sci. Rep.*, 2015, **4**, 4375.
23. C. Ding and A. S. Matharu, *ACS Sustainable Chem. Eng.*, 2014, **2**, 2217–2236.
24. N. Yousefi, X. Sun, X. Lin, X. Shen, J. Jia, B. Zhang, B. Tang, M. Chan and J.-K. Kim, *Adv. Mater.*, 2014, **26**, 5480–5487.
25. A. K. Roy, B. L. Farmer, V. Varshney, S. Sihn, J. Lee and S. Ganguli, *ACS Appl. Mater. Interfaces*, 2012, **4**, 545–839.
26. A. S. Kenyon and L. E. Nielsen, *J. Macromol. Sci. Chem.*, 1969, **3**, 275–295.
27. M. Aoki, A. Shundo, S. Yamamoto and K. Tanaka, *Soft Matter*, 2020, **16**, 7470–7478.
28. W. Zhao, S. L. Hsu, S. Ravichandran and A. M. Bonner, *Macromolecules*, 2019, **52**, 3367–3375.
29. L. Granado, S. Kempa, L. J. Gregoriades, F. Brüning, A.-C. Genix, J.-L. Bantignies, N. Fréty and E. Anglaret, *ACS Macro Lett.*, 2019, **8**, 984–988.
30. C. M. Sahagun and S. E. Morgan, *ACS Appl. Mater. Interfaces*, 2012, **4**, 564–572.
31. H. Kishi, T. Naitou, S. Matsuda, A. Murakami, Y. Muraji and Y. Nakagawa, *J. Polym. Sci., Part B: Polym. Phys.*, 2007, **45**, 1425–1434.
32. F. Meyer, G. Sanz, A. Eceiza, I. Mondragon and J. Mijović, *Polymer*, 1995, **36**, 1407–1414.
33. H. Mei, T. S. Laws, J. P. Mahalik, J. Li, A. H. Mah, T. Terlier, P. Bonnesen, D. Uhrig, R. Kumar, G. E. Stein and R. Verduzco, *Macromolecules*, 2019, **52**, 8910–8922.
34. G. E. Stein and T. S. Laws, *Macromolecules*, 2019, **52**, 4787–4802.
35. H. Matsuno, M. Totani, A. Yamamoto, M. Haraguchi, M. Ozawa and K. Tanaka, *Polym. J.*, 2019, **51**, 1045–1053.
36. S. Pruksawan, S. Samitsu, H. Yokoyama and M. Naito, *Macromolecules*, 2019, **52**, 2464–2475.
37. Y. Oda, *Polym. J.*, 2019, **51**, 955–962.
38. L. Zha, M. Zhang, L. Li and W. Hu, *J. Phys. Chem.*, 2016, **120**, 12988–12992.
39. S. Gupta, Q. Zhang, T. Emrick, A. C. Balazs and T. P. Russel, *Nat. Mater.*, 2006, **5**, 229–233.
40. K. Tanaka, T. Kajiyama, A. Takahara and S. Tasaki, *Macromolecules*, 2002, **35**, 4702–4706.
41. A. Yethiraj, *Phys. Rev. Lett.*, 1995, **74**, 2018–2021.
42. A. Hariharan, S. Kumar and T. Russell, *Macromolecules*, 1991, **24**, 4909–4917.
43. T. Hirai. K. Kawasaki and K. Tanaka, *Phys. Chem. Chem. Phys.*, 2012, **14**, 13532–13534.
44. M. Aoki, A. Shundo, K. Okamoto, T. Ganbe and K. Tanaka, *Polym. J.*, 2019, **51**, 359–363.
45. S. Yamamoto, R. Kuwahara, M. Aoki, A. Shundo and K. Tanaka, *ACS Appl. Polym. Mater.*, 2020, **2**, 1474–1481.
46. M. Aoki, A. Shundo, R. Kuwahara, S. Yamamoto, and K. Tanaka, *Macromolecules*, 2019, **52**, 2075–2082.
47. S. V. Kallivokas, A. P. Sgouros and D. N. Theodorou, *Soft Matter*, 2019, **15**, 721–733.
48. A. Izumi, Y. Shudo, K. Hagita and M. Shibayama, *Macromol. Theory Simul.*, 2018, **27**, 1700103.
49. M. S. Radue, V. Varshney, J. W. Baur, A. K. Roy and G. M. Odegard, *Macromolecules*, 2018, **51**, 1830–1840.
50. Y. Shudo, A. Izumi, K. Hagita, T. Nakao and M. Shibayama, *Polymer*, 2017, **116**, 506–514.
51. Y. Shudo, A. Izumi, K. Hagita, T. Nakao and M. Shibayama, *Polymer*, 2016, **103**, 261–276.
52. T. Okabe, Y. Oya and K. Tanabe, *Eur. Polym. J.*, 2016, **80**, 78–88.
53. A. A. Gavrilov, P. V. Komarov and P. G. Khalatur, *Macromolecules*, 2015, **48**, 206–212.
54. Y. Chen, J. Y. H. Chia, Z. C. Su, T. E. Tay and V. B. C. Tan, *Polymer*, 2014, **55**, 6124–6131.
55. T. Okabe, T. Takehara, K. Inose, N. Hirano, M. Nishikawa and T. Uehara, *Polymer*, 2013, **54**, 4660–4668.
56. N. Nouri and S. Ziaei-Rad, *Macromolecules*, 2011, **44**, 5481–5489.
57. P.-H. Lin and R. Khare, *Macromolecules*, 2009, **42**, 4319–4327.
58. P. V. Komarov, C. Yu-Tsung, C. Shih-Ming, P. G. Khalatur and P. Reineker, *Macromolecules*, 2007, **40**, 8104–8113.
59. D. Zhang, K. Li, Y. Li, H. Sun, J. Cheng and J. Zhang, *Soft Matter*, 2018, **14**, 8740-8749.
60. H. Sun, Z. Jin, C. Yang, R. L. C. Akkermans, S. H. Robertson, N. A. Spenley, S. Miller and S. M. Todd, *J. Mol. Model.*, 2016, **22**, 1–10.
61. H. Sun, *J. Phys. Chem. B*, 1998, **102**, 7338–7364.
62. M. Waldman and A. T. Hagler, *J. Comput. Chem.*, 1993, **14**, 1077–1084.
63. N. Kumar, S. Singla, M. C. Wilson, S. Kaur, S. Bekele, M. Tsige and A.Dhinojwala, *J. Phys. Chem. C*, 2019, **123**, 29729–29738.
64. N. Kumar, S. Kaur, R. Kumar, M. C. Wilson, S. Bekele, M. Tsige and A. Dhinojwala, *J. Phys. Chem. C*, 2019. **123**, 30447–30457.
65. S. Bekele and M. Tsige, *J. Phys. Chem. C*, 2018, **122**, 9015–9020.

 

66. C. Zhang, Y. Fujii and K. Tanaka, *ACS Macro Lett.*, 2012, **1**, 1317-1320.
67. M. Inutsuka, A. Horinouchi and K. Tanaka, *ACS Macro Lett.*, 2015, **4**, 1174-1178.

Table of Contents

Smaller molecules were preferentially segregated at the interface regardless of the epoxy and amine, and this segregation remained after the curing process.